
Wind-Driven Rain: From Theory to Reality

Hugo Hens, PhD
Fellow Member ASHRAE

ABSTRACT

Wind-driven rain (WDR) is known as a potentially damaging moisture source. Over the last decades, true advances in predicting WDR's impact on building enclosures have been made. Computational fluid dynamics (CFD)-based windfield calculations, in combination with droplet trajectory tracing, allowed for calculation of catch-ratio distributions. Validation comparison with measured data showed results to be quite close to observations. Bouncing, splashing, evaporation, and buffering—phenomena occurring when raindrops strike a surface—also were analyzed.

Actual HAM-models handle WDR as a flow rate that is either (1) buffered by a capillary active outside finish until run-off starts once its surface has turned capillary wet or (2) runs off immediately if the finish is noncapillary. The absorbed part of the run-off is redistributed while drying to the outside and the inside. During sunny weather, solar-driven diffusion activates redistribution, causing high relative humidity sorption and sometimes interstitial condensation in and against layers close to the inside finish. At the design stage, one could expect these model capabilities to help predict problems with the proposed enclosure solution. This, however, is hardly true. What happens with run-off is too random and circumstantial to be grasped by models, as this paper illustrates using three real-world cases.

INTRODUCTION

Buildings contend with several moisture sources. Built-in moisture, rising damp, rain, water heads, and accidental leaks manifest as liquid water, whereas water vapor contributes to sorption, surface condensation, and interstitial moisture deposits. Rising damp may cause severe damage but is easily avoided. Built-in moisture should dry without annoyances. Preventing accidental leaks requires good design and construction and proper maintenance. Sorption by interior finishing layers is not a problem as long as relative humidity indoors remains between 30% and 65%.

What's left as potentially damaging moisture sources are rain, surface condensation, and interstitial moisture deposits. Preventing surface condensation in cold and cool climates demands high enough thermal resistances, absence of problematic thermal bridges and correct ventilation. In hot and humid climates, air drying using dedicated outdoor air systems

(DOAS) is the way to go. In cool and cold climates, interstitial moisture deposits cause trouble in enclosures that are too air permeable; whereas in buildings with high vapor release indoors, problems may already arise when vapor diffusion resistances across the enclosure assemblies increase from inside to outside. In hot and humid climates, where cooling is needed, outdoor airflow must be counteracted, while vapor diffusion resistances must increase from inside to outside (Trechsel 2001).

In calm (i.e., windless) weather, raindrops fall vertically. In wind, raindrop paths are oblique; the vertical component is called *precipitation* and the horizontal component is called *wind-driven rain* (WDR). While precipitation wets horizontal and sloped surfaces, wind-driven rain also humidifies vertical surfaces. The amount of water striking an enclosure in this way makes wind-driven rain a potentially damaging moisture source (Mumovic et al. 2009).

Hugo Hens is a professor emeritus in the Department of Civil Engineering, Unit of Building Physics, University of Leuven (K.U. Leuven), Leuven, Belgium.

THEORY AND RESEARCH REVIEWED

Wind-Driven Rain Striking a Building Enclosure

Quantification of wind-driven rain began in the 1950s with R.E. Lacy (1951). From measurements with rain gauges on facades in Thorntonhall, Scotland, and Garston, England, and using an empirical relation between median drop size, precipitation intensity, and terminal drop speed (Laws et al. 1943; Best 1950), he deduced the following free-field formula (Lacy 1964):

$$g_{WDR} = 0.222v_w g_{PREC}^{0.88} \quad (1)$$

where

g_{WDR} = average wind-driven rain intensity, $\text{kg}/(\text{m}^2 \cdot \text{s})$

v_w = average wind speed, m/s

g_{PREC} = average precipitation intensity in $\text{kg}/(\text{m}^2 \cdot \text{s})$

All variables were logged during the same period of time. A simplified version of Equation 1 is as follows:

$$g_{WDR} = 0.2v_w g_{PREC} \quad (2)$$

Thus, WDR intensity increases with higher wind speed. For speeds beyond 5 m/s, WDR free-field intensity even surpasses precipitation intensity. The product of precipitation and wind speed in Equation 2 is called the *wind-driven-rain index*.

Each environment and each individual building, with its orientation, form, enclosure design, and shielding details, distorts the windfield and causes WDR striking the façade to differ from the free-field intensity. As a result, Equation two must be modified as follows:

$$g_{WDR} = [(0.2C_{WDR} \cos \theta)v_w]g_{PREC} \quad (3)$$

where C_{WDR} is the WDR factor and θ is the angle between wind direction and the surface considered. The product in brackets is called the *catch ratio* η , whereas the product in parentheses gives the *WDR factor* a , both for a given spot on a facade. British Standards Institution standard *BS 8104, Code of Practice for Assessing Exposure of Walls to Wind-Driven Rain* (BSI 1992; Sanders 1996) lists the wind driven rain factor as the product of a topography factor T , a terrain roughness factor R , an obstruction factor O , and a wall factor W :

$$C_{WDR} = TROW \quad (4)$$

Equation 3 has been tested by several authors (Lacy 1951, 1964; Holmgren 1972; Sandberg 1974; Isaksen 1975; Künzel 1976; Straube 1998; Straube and Burnett 2000; van Mook 2003; Blocken 2004; Nore 2005; Brüggen et al. 2009). An experiment measuring the WDR factor also ran on a building with a low-slope roof at the KAHO Campus in Gent, Belgium, from December 2, 1992 until the end of January 1993 (Hens et al. 1994). Three of the four façade walls were equipped with rain gauges (Figure 1):

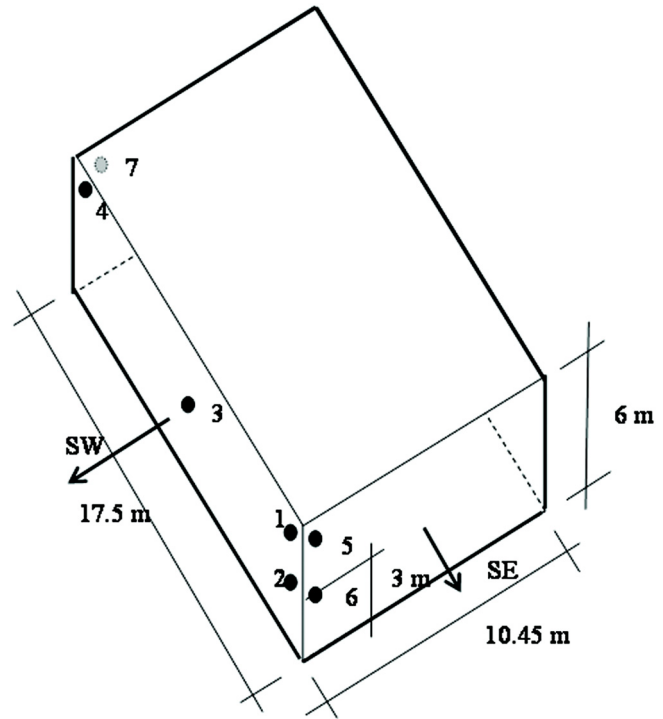


Figure 1 Building at KAHO, Gent, Belgium, used for the WDR measurements: dimensions, orientation, and location of the rain gauges

- One at the upper-right corner of the wall facing southwest (Gauge 1)
- One at the middle of the right side of the wall facing southwest (Gauge 2)
- One at the middle of the wall facing southwest (Gauge 3)
- One at the upper-left corner of the wall facing southwest (Gauge 4)
- One at the upper-left corner of the wall facing southeast (Gauge 5)
- One at the middle of the left side of the wall facing southeast (Gauge 6)
- One at the upper-right corner of the wall facing northwest (Gauge 7)

The southwest wall was 17.5 m long, the walls facing southeast and northwest were 10.45 m long, and all three were 6 m high. Precipitation was measured on a grass field close to the building, while wind data came from the nearest weather station. Table 1 summarizes the results. Figure 2 shows the data and least-square line for Gauges 1 (worst correlation) and 5 (best correlation). The results underline the large variation in WDR factors along an enclosure, with the edges facing the main wind direction being the most exposed.

A second experiment, now measuring the catch ratio, was conducted in Leuven, Belgium, on the three façades of a

Table 1. Test Building at the KAHO Site*

Rain Gauge	$g_{WDR} = av_w g_{PREC}$		
	Wind-Driven Rain Factor (a)	Stadev (a)	r^2
1	0.116	0.016	0.19
2	0.066	0.007	0.34
3	0.075	0.009	0.28
4	0.085	0.011	0.30
5	0.041	0.006	0.41
6	0.023	0.004	0.38
7	0.031	0.007	0.19

* Relation between the daily wind-driven rain intensity impinging on each of the seven spots and the daily wind-driven rain factor measured close to the building site.

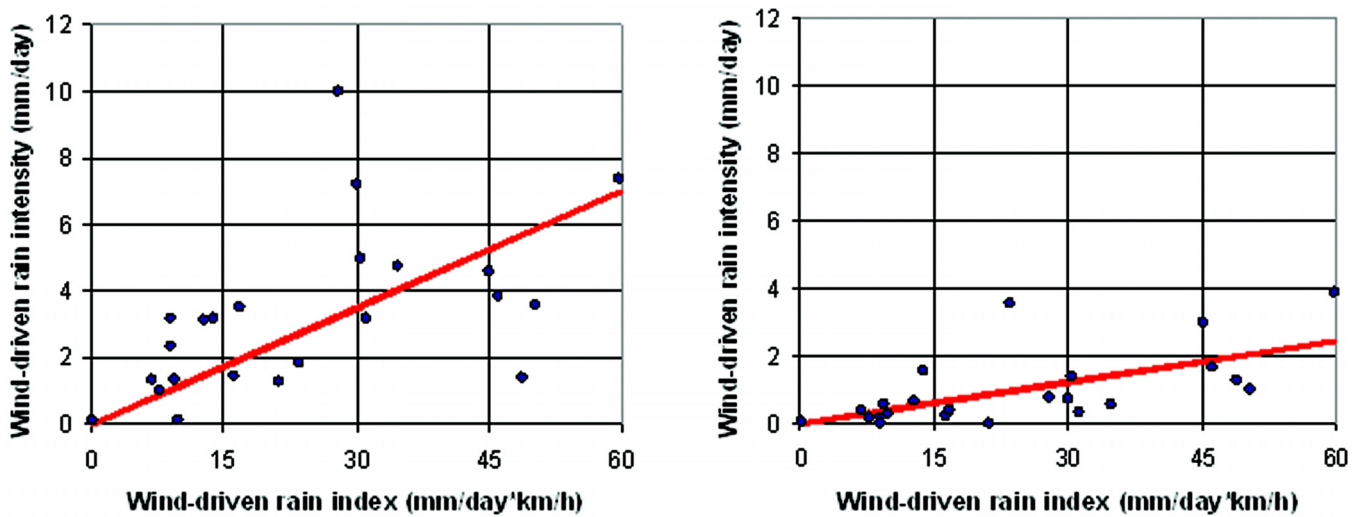


Figure 2 Building at KAHO, Gent, Belgium—Relation between WDR index and WDR, measured with the rain gauges. Left gauge 1 shows the worst correlation, right gauge 5 shows the best correlation.

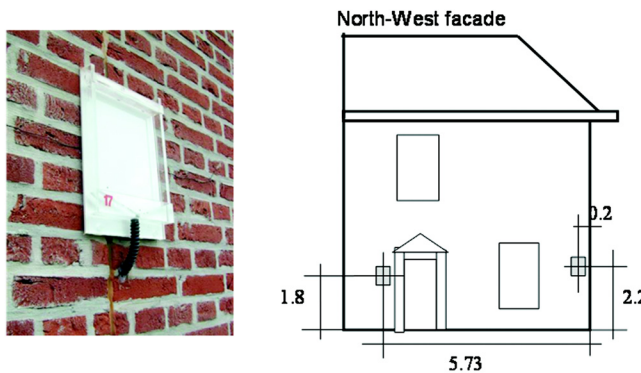


Figure 3 Two-family house in Leuven, Belgium: Northwest façade with location of the rain gauges.

two-family house (Figure 3). Table 2 lists the results. Also here, a large variation is noted with highest value close to the edge of the southwest façade, the one looking to the main wind direction (Mohamed 1992).

The first attempts to calculate WDR distribution on building enclosures dates from the early 1970s (Sandberg 1974; Rodgers 1974). Predictions were based on a combination of wind tunnel measurement and raindrop-trajectory tracing using Newton’s law for force equilibrium between gravity, wind drag, and inertia. The buildings considered were infinitely long. Results showed a concentration of rain at the top, which showed good agreement with measurements made on buildings in Gothenburg and Stockholm, Sweden.

With increasing computer power, computational fluid dynamics (CFD) became feasible, and in the nineteen eighties

Table 2. Two-Family House in Leuven*

Location	NW 5.7/1.8 m	NW 0.2/2.25 m	SW 0.2/2.25 m	SW 5.7/1.8 m	NE 1.7/2.25 m	NE 4.4/2.7 m
Catch Ratio, η	0.016	0.26	0.23	0.047	0.008	0.014

* Measured Catch Ratio (η) northwest and southwest at a height of 2.25 m, 0.2 m from the edge, and a height of 1.8 m, 5.73 m from the edge, catch ratio northeast.

researchers began predicting wind flow fields around buildings by combining CFD with different turbulence models (Häggkvist et al. 1989). From the early 1980s, linking CFD to rain drop trajectory tracing allowed calculation of steady-state WDR impact on building enclosures (Choi 1993; Karagiozis and Hadjisophocle 1996; van Mook 2003; Blocken 2004; Blocken et al. 2007). Continuous mapping of average catch ratios became possible, an advancement compared to earlier spot-wise experiments and simplified calculations. A few validation exercises comparing calculated to measured catch ratios turned out to be quite positive (Blocken and Carmeliet 2002; Nore 2005). In the time since, ample calculation results confirm earlier experimental and simplified model findings: highest average catch ratios at the top along the top edges of façades facing the wind, low catch ratios in the façades' middle and lower parts, and catch ratios hardly different from zero on facades oriented away from the wind. At higher WDR intensities, catch ratios were found to be equalized over the façade facing the wind. Projections proved effective at shedding part of the façade below, a benefit often forgotten by today's architects when designing prestigious buildings. A full, dynamic WDR calculation, including wind gusts and varying wind direction, is still out of scope.

What Happens When Raindrops Strike a Surface

Raindrops that strike a surface are supposed to be absorbed or run off. Absorption is the safest of these two mechanisms in terms of avoiding unwanted consequences, with only two phenomena potentially affecting moisture tolerance: (1) solar-driven vapor flow and (2) moisture transmitted by capillarity to layers inside the enclosure. The first mechanism may cause high relative humidity sorption in layers close to the inside and result in interstitial condensation on noncapillary layers. Avoidance demands inner layers with high moisture buffer capacity, such as a masonry leaf, or a correct sequence of vapor diffusion resistances between the absorbing veneer or siding and the finishing layer inside. The second mechanism is easily stopped by inclusion of an air cavity or the use of a noncapillary layer behind the capillary veneer or siding. Run-off has a much higher potential of putting moisture tolerance at risk. Wind can press the water film through cracks hardly wider than 0.15 mm, whereas water heads in vertical joints and above badly flashed projections easily cause leakage.

A simple line of reasoning in favor of absorption starts by stating that drops touching a capillary siding or veneer wall cause a one-dimensional moisture flow in the material, perpendicular to the surface. Suppose w_{cr} is the critical mois-

ture content of the material in kg/m^3 . Above, capillary flow starts; below, only equivalent vapor diffusion intervenes. Absorption depth in the material is at any moment given by (Hens 2007):

$$x = \frac{A^2 w_{cr}}{g_{WDR}(w_c^2 - w_{cr}^2)} \left(\sqrt{1 + \frac{2g_{WDR}^2(w_c^2 - w_{cr}^2)t}{A^2 w_{cr}^2}} - 1 \right) \quad (5)$$

where A is the capillary water absorption coefficient in $\text{kg}/(\text{m}^2 \cdot \text{s}^{0.5})$ and w_c is the capillary moisture content in kg/m^3 of the material used. As absorption depth grows, moisture content at the exterior surface increases according to

$$w = w_{cr} + \frac{g_{WDR}(w_c^2 - w_{cr}^2)x}{A^2} \quad (6)$$

When that value touches capillary moisture content during a rain event, absorption blocks and run-off starts.

Both formulas show that impinging WDR intensity, capillary properties of the material used (A , w_c) and thickness (x) of the siding or veneer wall fix the maximum absorbed before run-off starts. A 9 cm thick veneer wall built with bricks that have a high capillary absorption coefficient and high capillary moisture content is a very effective absorbent. Onslaught to run-off requires hours of downpour or days-long drizzle. Contrary to that, concrete block veneers, stucco, timber siding, vinyl siding, and metal siding are hardly capillary to noncapillary, so onslaught to run-off develops quickly, even instantaneously.

More advanced research on what happens globally when rain droplets strike a surface goes back to the nineteen fifties. The main phenomena beside absorption observed in that time were splashing and evaporation. Couper (1974) reported on an exploratory study at CSIRO in Australia. As Table 3 shows, three surface conditions seem to define splashing: roughness, water repellence, and wetness.

Couper also looked to the shedding effectiveness of projections. Discharge was most effective if projections extended far enough (up to 40 mm was tested), sloped away from the façade, and had a drip edge. Later, run-off fingering as observed on vertical walls was analyzed. The reason for this cause of inhomogeneous soiling seemed attributable to competing capillary and gravity forces, induced by variations in the surface's porous structure (Küntz and van Mier 1997). Beyond 2000, additional attempts were made to relate surface soiling to WDR impingement (Blocken et al. 2003). Some researchers also studied shedding efficiency of metal flashing and parapet flashing and showed that small changes in design had a major impact on it (Saneinejad et al. 2006; Kvande and

Table 3. Average Splash Factors for Four Surfaces (Couper 1974)

Material	Surface Characteristic	Splash Factor	
		Dry	Wet
Sheet glass	Clean, polished, hydrophilic	0	2
Sheet acrylic	Clean polished, water repellent	24	25
Sand-epoxy resin coating on substrate	Smooth rendered	13	17
River gravel-epoxy resin on substrate	Rough	11	18

Liso 2009). Abaku (2009) analyzed splashing, bouncing, and spreading experimentally and was one of the first to simulate absorption and evaporation of individual raindrops striking a vertical surface. The differences with the continuous flow rate approach were not negligible.

Benefits for Designers and Builders

Designers and builders clearly benefitted from the theory developed and the research done. Some insights gained have already been mentioned: the positive effect of projections, the advantage of buffering compared to nonbuffering outside layers, stopping absorbed rainwater redistribution, and assembling façade walls so as to avoid problems with solar-driven vapor diffusion. Applied research also fixed the three outside wall assembly types, which assured rain-tightness:

1. Massive brick walls, thick enough to act as safe capillary buffers (never more than half the thickness wetted by rain). Before the advent of cavity walls, such walls were the preferred façade construction in Northwestern Europe (Schnapauff et al. 1993).
2. Cladding the walls with a rain-tight siding or water-repellant stucco, so turning its outside surface into a nonbuffering drainage plane. This option demands careful design of joints around windows, doors, coping stones, etc.
3. A rain screen solution where the outside cladding or veneer is backed by an air cavity or a water-repellant layer and where the inside leaf cares for airtightness. Two drainage planes are created this way, one at the outside surface and one at the cavity or water-repellant layer side. Run-off along the second drainage plane must be prevented from reaching the inside leaf, which is the reason why trays are inserted at the bottom of the cavity or water-repellant layer, and holes are inserted in the veneer wall or siding so that collected run-off is drained to the outside (CMHC 1987; Hens 2007). The rain-screen solution, being the most rain tolerant, gained preference over the other two, especially in regions with high WDR intensities.

USABILITY OF HEAT-AIR-MOISTURE SOFTWARE AS A DESIGN TOOL

Though not perfect (see the continuous flow rate assumption), the impact of rain absorption on the hygrothermal

response of enclosure parts is well approximated by the actual heat-air-moisture computer models. However, predicting what happens on and in enclosures once run-off develops and assessing future soiling, leakage, and rain penetration, considering all enclosure details, remains out of scope. Figure 4 shows how a 1×1 m² large concrete block veneer turns wet at its cavity side during a run-off laboratory test, whereas Figure 5 gives the overall and cavity-side run-off measured on a 1.8 m wide and 2.7 m high concrete block veneer exposed to a moderate but wet outside climate.

No software is able to simulate these random test results; the reasons for this are manifold. Even three-dimensional codes simplify the geometry of an assembly compared to reality, as they can not anticipate the randomness and real geometry of cracks, leaks, and accidental air layers, nor can they match the specificity of each detail. Building materials are further considered as being homogeneous, though they are not. Between material layers, ideal suction contact is assumed, while in reality suction, diffusion, and drained and mixed contacts are possible. For layers in suction contact, the contact zone often has properties that differ from the materials in contact (Brocken 1998; Qiu 2003). Most models cannot handle gravity and pressure heads, although both are the main driving forces behind rain leakage when run-off occurs. The outdoor climate is also typically averaged on an hourly basis, while WDR demands much shorter time steps.

As a consequence, information on rain penetration and the damages caused still must come from experimental work and the evaluation of real-world cases.

THREE EXAMPLES OF REAL-WORLD CASES

The three examples that follow illustrate the importance of real-world-case evaluations to understanding the damage WDR can cause. Despite the impossibility of full modeling, these cases show that physics contributes to an understanding of why problems occur and how they can be avoided in future designs.

Case 1: Hotel at the Coast

The Belgian coastline faces northwest, with most WDR coming from south over west to northwest. The main façade of the hotel under scrutiny faces southwest. The building has a trapped structure in which each floor regresses from the one below, allowing all rooms to have a large balcony not shadowed

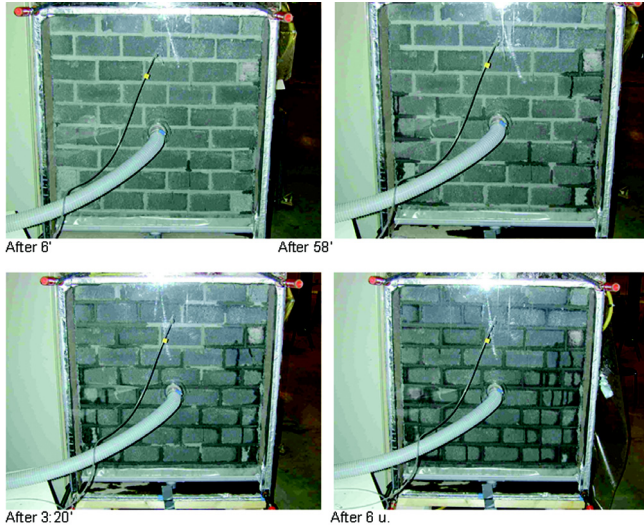


Figure 4 Run-off test in the laboratory: Time evolution of the rain penetration at the cavity side of a concrete block veneer.

by the one above (Figure 6a). As a consequence, each balcony acted as a rain gauge. The façade consisted of a cavity wall with a 9 cm thick concrete block veneer, a 3–4 cm wide unfilled cavity, and a 14 cm thick nonplastered concrete block inside leaf. The veneer blocks showed no capillary activity, whereas their 9 cm height made a full mortar fill of the head joints during block-laying difficult, which resulted in mortar drops in the cavity and debris accumulation on the tray (Figure 6b). Over time, microcracks also formed between the pointed head joints and the concrete blocks. Coping stones covering the hollow walls along the balconies had no watertight layer below that stopped rain from penetrating and leaking into the hollow.

Each WDR event caused run-off along the outside surface of the noncapillary veneer. Wind and gravity allowed that run-off to easily penetrate the veneer’s mortar joints. When not plastered on the inside, concrete block leaves are not air-tight. As a result, rain water running off along the veneer’s cavity side was blown across the cavity and humidified the inside leaf. At the same time, the mortar debris on the trays allowed the run-off at the cavity side to reach the inside leaf. Since rain barriers were not installed along the windows where the veneer touched the separation wall between the rooms (Figure 6c), rain water also moistened the window reveals. Rain also leaked into the hollow walls along the balconies.

The floors consisted of prefabricated concrete elements whose horizontal hollows touched the veneer wall. As a result, cavity-side run-off could enter these elements and collect at the floor’s lowest point in the center of each room.

The consequences were dramatic. During WDR events, run-off started immediately and caused rain to penetrate the

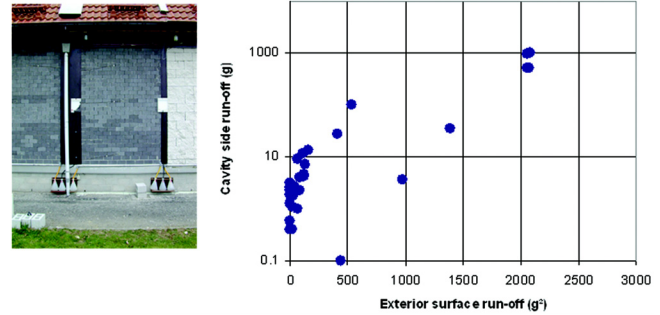


Figure 5 Filled cavity wall with concrete block veneer exposed to WDR at the test building of LBF, K.U. Leuven, Belgium—Relation between the WDR impacting the veneer and run-off at the cavity side collected at the cavity tray



Figure 6 Hotel at the Belgian coast: (a) the building, (b) tray short-circuited by mortar debris, (c) lack of a watertight layer where the veneer touches the inside walls, (d) wet inside leaf, (e) surface condensation on double glazing, (f) final retrofit

veneer, cross the cavity, moisten the inside leaf, and humidify large parts of the inside surface (Figure 6d). At the same time, water dripped out of the floor at the central light in each room

and wetted the bed below. Drying, in turn, elevated the relative humidity inside, causing surface condensation on the double-glazed windows during colder weather (Figure 6e).

Remarkably, the forensic expert flagged interstitial condensation at the cavity side of the veneer wall by water vapor diffusion as cause of the problems. This was verified by covering one of the side façades with a polyethylene-sheet, assuming that if diffusion was the cause, condensation would appear at the backside of that sheet. This was the case, not as a consequence of diffusion-based interstitial condensation, but because the cavity wall was wet by rain leakage and dried partly to the outside.

The problem was addressed by cladding the existing façade with a new rain-tight layer composed of factory-made fiber-cement elements (Figure 6f). The costs were impressive, though lower than they would have been if the veneer wall had to be removed, all trays cleaned, rain barriers added where needed, the veneer brick-laid again, and the inside leaf plastered.

It was not possible to predict the cause of the problem by using the actual HAM-models, as the main causes were run-off, gravity-induced leakage at the head joints and the coping stones, collection of cavity run-off on the trays piled with debris, wind-induced droplet spray across the cavity, etc. Nevertheless, many lessons were learned: (1) use capillary active veneer walls (on the condition that the inside leaf has a high moisture buffer capacity); (2) apply correctly mounted, sealed trays; (3) avoid mortar debris falling into the cavity and collecting on the trays; (4) care for air tightness of the inside leaf when designing a cavity wall; (5) avoid leaky coping solutions; and (6) close the hollow channels in prefabricated floor elements that face the veneer.

Case 2: University Building

The university building scrutinized housed a very diverse program: underground parking, lecturing theatres, a library, smaller seminar rooms, and individual offices. For this reason, the design team proposed a building that narrowed from basement to top. The lecture theatres were situated just above the underground parking. The library was posted above the parking, while the seminar rooms and offices filled the higher floors. The result was a building with oblique façade walls (Figure 7a). These were solved as cavity walls with a 9 cm thick masonry veneer, a cavity partially filled with PUR-boards, and a 14 cm thick reinforced concrete inside leaf with brick finish indoors.

The main complaint of the university council and the building users was the appearance of large moisture spots on the inside surface of the oblique cavity walls. A second complaint concerned rain penetration along most window sills at the upper floors (Figures 7b and 7c). Soon after the building was finished, the oblique veneer wall buckled locally. It underwent a provisional repair that stood for years. In an early trial to stop humidification of the inside surface, the veneer was treated with a water-repellant agent.

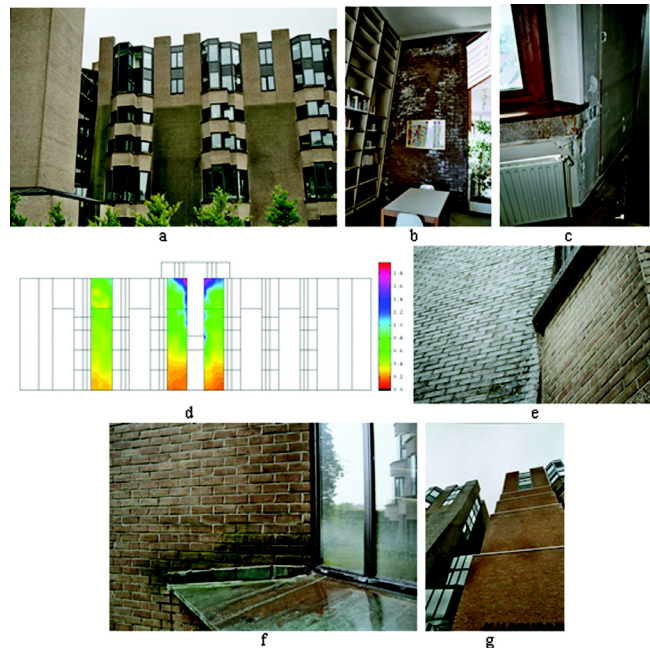


Figure 7 University building: (a) view of the building, (b) wet spots and efflorescence on the inside brick finish, (c) leakage at the windows, (d) WDR impact calculated with CFD/RDTT software, (e) WDR run-off along the oblique veneer wall, (f) rain wetting the window sills, and (g) the first mismatched retrofit.

The cause of the moisture spots was easily diagnosed as precipitation and wind-driven rain running off along the oblique veneer wall. A more detailed analysis was made to confirm that diagnosis. The catch-ratio pattern on the building envelope for WDR coming from the main wind direction (southwest) was calculated using CFD in combination with rain-drop trajectory tracing. These showed heavy exposure to WDR (Figure 7d), to which precipitation had to be added.

Run-off was analyzed on-site, proving that the oblique façades functioned as very active drainage planes with a clear concentration of run-off at the edges (Figure 7e). As the veneer was water repellent, the main run-off load was put on the interfaces between bricks and mortar. Even without water-heads, obliqueness allowed gravity to cause leakage through the cracks into the cavity. The leaking water dripped onto the insulation, ran-off, penetrated the joints between the insulation boards, and wetted the concrete inside leaf, where shrinkage cracks directed the water to the brick-finished inside. Rain penetration along the window sills required no extended study. It was caused by the lack of sill steps below the window frames (Figure 7f).

Repair, however, was a different story. In an early trial, one of the oblique veneer walls was replaced by a stepwise

regressing veneer (Figure 7g). The view was awful. The solution also introduced thermal bridging, which lifted the whole wall U-factor from 0.49 to 0.64 W/(m²·K). Trays at the bottom of the veneer at each step were forgotten, leaving room for further leakage. The solution finally proposed was exchanging the brick veneer for a watertight zinc cladding on timber lathing, which solved the sill problem and did not create thermal bridges. Run-off was collected in gutters down each cladding and drained to the sewage system. Costs, however, were so high that the council finally decided to quit the building.

It was possible to predict the outcome for the catch-ratio distribution along the enclosure using the WDR and heat-air-moisture models available, though the impact of precipitation was not determined this way. Also the leakage paths were too random to be understood correctly. Despite this lack of predictability, physics contributed to an understanding of why leakage was so disastrous: water repellency destroying the bricks as capillary active layer, run-off load concentrated on the joints, gravity active thanks to the obliqueness of the veneer walls. The two main lessons learned from the case were: (1) oblique masonry walls are a demand for rain penetration problems if the veneer is not water-tight and (2) sills need a slope away from and a step up below the window to function properly. Otherwise, wind may blow the rain between window and sill to the inside, a fact not covered by models.

Case 3: Detached House

The house, constructed in 2003, has two floors, an attic and a basement. The structure consists of load-bearing brickwork with concrete slabs in prefabricated elements, beams where needed, and columns to support concentrated loads. The façade cavity wall has a veneer, brick-laid with 9 cm thick sand-lime stones at the second floor and constructed of stone elements with thickness 3 cm at the first floor; an 11 cm wide cavity filled with 10 cm glass-fiber bats; and an inside leaf in perforated large blocks, plastered at the inside. According to the design documents, a watertight layer was inserted above the basement walls just below the ground floor slab (Figure 8a), while all cavities had trays above that slab and above the low-sloped roof covering part of the living room. The owners nevertheless complained about rain penetration in the basement, rain leakage in the living room, and some rising damp in one of the sleeping rooms lining up along the low-sloped roof above the living room.

Problems were related specifically to the southwest façade, which faced the main WDR direction. The garden that façade looked too was flat, so rain collected there could not reach the building and sink in the ground fill around the basement. A closer look revealed that rain penetrated between the ground floor slab and the watertight layer below (Figure 8b). That turned the attention to the cavity walls above. Below the veneer, the watertight layer protruded a little to the outside. Sand-lime stone and the stone used were hardly capillary. Wind-driven rain thus quickly caused water run-off (Figure 9), building up a water head on the protrusions, high enough to



Figure 8 *New detached house: (a) watertight layer between basement wall and concrete floor elements, (b) run-off in the basement along the exterior below grade walls, (c) poor flashing down the filled cavity wall above the low-sloped roof covering part of the living room, and (d) wrongly mounted tray down the filled cavity of that wall.*

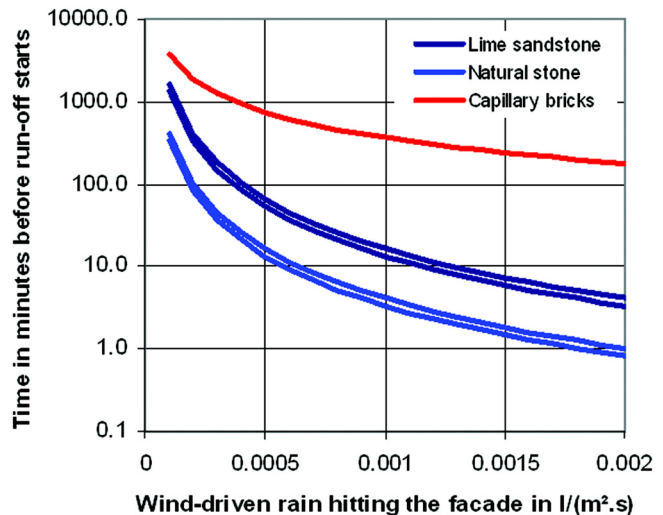


Figure 9 *Simplified modeling: time delay between the start of a WDR event with given intensity and the moment run-off begins.*

push the rain between the watertight layer and the slab above to the basement's inside, where it flowed down the walls. For such outflow to happen, water heads are needed. In fact, when capillarity acted as sole driving force for the water reaching the

inside, the menisci that activate suction should have flattened there, stopping water to move and leak.

Leakage in the living room and the damp spots in the sleeping rooms were caused by bad flashing and bad tray detailing down the filled cavity at the low-sloped roof above the living room (Figures 8c and 8d). That leakage may not have occurred if a capillary brick veneer was used. In fact, the hardly capillary sand-lime stone aggravated rain water penetration through the head joints. Subsequent cavity run-off collected at the failing tray, where it found its way to the inside.

The solution proposed was simple. The stone veneer received a projected drip-nose just above the watertight layer, and the lime-sandstone veneer was opened block-wise to cure the tray problems.

It was not possible to predict what happened using the heat-air-moisture models available. Without a true physical understanding, the situation could not be explained. Also, some of the lessons learned in Case 1 were confirmed: (1) use capillary active veneer walls and (2) apply correctly mounted, sealed cavity trays.

CONCLUSION

Wind-driven rain is the subject of extended experimental and theoretical work. The achievements of this work are impressive. The combination of CFD and raindrop-trajectory tracing allows prediction of the average catch-ratio distribution over building enclosures with acceptable accuracy, as validation shows. What happens when rain drops strike a surface has been studied in detail. How wall assemblies should be constructed to ensure rain-tightness is addressed. The effects of absorbed rain water in wall assemblies are acceptably well estimated using the actual heat-air-moisture computer tools. However, run-off presents complexity that cannot be addressed by actual models, which leaves practice as the primary learning environment.

The three cases presented show that physics contributes to an understanding of what happens and what should be done to avoid problems. Lessons learned include the following:

- Use capillary active veneers (on condition that the inside leaf has a high moisture buffer capacity, which is not the case with timber-framed inside leaves).
- Apply correctly mounted and sealed trays; avoid mortar debris falling into the cavity and collecting on top of the trays.
- Care for air tightness when designing the inside leaf.
- Avoid leaky coping solutions.
- Close the hollow channels in prefabricated floor elements that face the veneer.
- Never construct oblique cavity walls with rain screens that are not water tight, and do not forget run-off management if veneers lack capillarity.

REFERENCES

- Abaku, M. 2009. Moisture stress of wind-driven rain on building enclosures. PhD thesis, K.U. Leuven.
- Best, A.C. 1950. The size distribution of raindrops. *Quarterly Journal Royal Meteorological Society* 76:16–36.
- Blocken, B., J. Carmeliet. 2002. Spatial and temporal distribution of driving rain on a low-rise building. *Wind & Structures* 5(5):441–62.
- Blocken, B., W. Desadeleer, and J. Carmeliet. 2003. Numerical study of façade disfigurement by driving rain. *Proceedings of the Second International Building Physics Conference*, Carmeliet, Hens, and Vermeir, eds. Leuven, Belgium: Balkema Publishers.
- Blocken, B. 2004. Wind-driven rain on buildings, measurement, numerical modeling and applications. PhD thesis K.U. Leuven.
- Blocken, B., S. Roels, and J. Carmeliet. 2007. A combined CFD-HAM approach for wind-driven rain on building facades. *Journal of Wind Engineering and Industrial Aerodynamics* 95(7):585–607.
- Brocken, H.J.P. 1998. Moisture transport in brick masonry: The grey area between bricks. PhD thesis, TU/e, Eindhoven.
- Briggen, P.M., B. Blocken, and H.L. Schellen. 2009. Wind-driven rain on the façade of a monumental tower: Numerical simulation, full-scale validation and sensitivity analysis. *Buildings and Environment* 44:1675–90.
- BSI. 1992. British standard code of practice for assessing exposure of walls to wind-driven rain. BS8104, British Standard Institution.
- Choi, E.C.C. 1993. Simulation of wind-driven rain around a building. *Journal of Wind Engineering and Industrial Aerodynamics*. 46:721–29.
- CMHC. 1987. Moisture problems. Builder's series.
- Couper, R.R. 1974. Factors affecting the production of surface run-off from wind-driven rain. Proceedings of the Second International Symposium on Moisture Problems in Buildings, Paper 1.1.1.
- Häggkvist K., U. Svensson, R. Taesler. 1989. Numerical simulations of pressure fields around buildings. *Building and Environment* 26(1):65–72.
- Hens, H., and A.F. Mohamed. 1994. Preliminary results on driving rain estimation, IEA-ECBCS-Annex 24, Report T2-B-94-02.
- Hens, H. 2007. Building Physics: Heat, Air and Moisture: Fundamentals and Engineering Methods with Examples and Exercises. Berlin: Ernst & Sohn.
- Hens, H., A. Janssens, W. Depraetere, J. Carmeliet, and J. Lecompte. 2007. Brick cavity walls: A performance analysis based on measurements and simulations. *Journal of Building Physics* 31(2):95–124.
- Holmgren, O. 1972. Snow loads, driving rain and building design. Colloquium, "Teaching the teachers on building climatology", Statens Institut for Byggnadsforskning, Stockholm, Preprint no 35.

- Isaksen, T. 1975. Driving rain in Bergen, Norwegian Building research Institute F4625, Trondheim, Norway.
- Karagiannis, A., and G. Hadjisophocleous. 1996. Wind-driven rain on high-rise buildings. *Proceedings of the Thermal Performance of Exterior Envelopes of Buildings VI, Clearwater Beach, Florida*.
- Küntz, M., J.G.M. van Mier. 1997. Field evidences and theoretical analysis of the gravity-driven wetting front instability of water runoffs on concrete structures. *Heron* 42(4):231–44.
- Künzel, H. 1976. Beurteilung der Schlagregenbeanspruchung und des Regenschurzes von Gebäuden, IBP-Bericht B.Ho5/76 (in German).
- Kvande, T., and K.R. Liso. 2009. Driving-rain protective design of parapet flashing. *Proceedings of the Fourth International Building Physics Conference, "Energy efficiency and new approaches," Istanbul, Turkey*, pp 193–200.
- Lacy, R.E. 1951. Distribution of rainfall around a house, *Meteorological Magazine* 80:184–89.
- Lacy, R.E. 1964. Driving rain at Garston, UK, CIB Bulletin, no 4, pp. 6–9.
- Laws, J.O., and D.A. Parsons. 1943. Relation of raindrop size to intensity *Transactions of the AGU* 24(2)453–60.
- Mohamed, A.F., O. Nejat, and H. Hens. 1992. Outdoor climate: Reference year, driving rain. EA-ECBCS-Annex 24, Report T2-B-92-05.
- Mumovic, D., and M. Santamouris. 2009. *A Handbook of Sustainable Building Design and Engineering: An Integrated Approach to Energy, Health and Operational Performance*. London: Earthscan Ltd.
- Nore, K. 2005. Measurements of driving rain dispersion on a low-rise test building in Norway. IEA-ECBCS-Annex 41, Report A41-T3-N-05-2.
- Qiu, X. 2003. Moisture transport across interfaces between building materials. PhD thesis, Concordia University, Montreal, Quebec.
- Rodgers, G.G., G. Poots, J.K. Page, and W.M. Pickering. 1974. Rain impaction on a slab type building: A theoretical approach. *Proceedings of the Second International Symposium on Moisture Problems in Buildings*. Paper 1.1.3
- Sandberg P.I. 1974. Driving rain distribution over an infinitely long, high building: computerized results, *Proceedings of the second international symposium on moisture problems in buildings*, paper 1.1.2.
- Sanders C. 1996. IEA-ECBCS Annex 24: Heat, Air and Moisture Transfer in Insulated Envelope Parts, Final Report task 2, Environmental Conditions, ACCO, Leuven, ISBN 90-75741-03-0, 96 p.
- Saneinejad S., Doshi H., Horvat M. 2006. Test method to study the water shedding effectiveness of drip-edge of metal flashing, *Proceedings of the third international building physics conference 'Research in building physics and building engineering'* ed. Fazio, Hua Ge, Rao & Desmarais, Taylor & Francis, Montreal, 27-31 August, pp 411–17.
- Schnapauff V., Dahmen G., Oswald R. 1993. Schlagregenschutz von Aussenwänden, zur Bewährung und Beurteilung wasseraufnehmender Fassadenkonstruktionen, Referat BI5, *Bauforschungsberichte des Bundesministers für Raumordnung, Bauwesen und Städtebau*, IRB-Verlag, 77 p.
- Straube J. F. 1998. Moisture control and enclosure wall systems, PhD-thesis, University of Waterloo, 318 p.
- Straube J.F., Burnett E. F. P. 2000. Simplified prediction of driving rain on buildings, *Proceedings of the International Building Physics Conference*, Eindhoven, pp 375-382.
- Trechsel H. 2001. Moisture analysis and condensation control in building envelopes, ASTM Manual MNL 40, American Society for Testing and Materials, West Conchohocken, PA.
- Van Mook F.J.R. 2003. Driving rain on building envelopes, PhD-Thesis TU/e, Eindhoven, 198 p.